*Proceedings of the*
*Annual Stability Conference*
*Structural Stability Research Council*
*San Antonio, Texas, March 21-24, 2017*

# Effects of soil support on the stability of corrugated metal pipe

P. Graham Cranston[1], Matthew C. Richie[2], Luiz C. M. Vieira, Jr[3]

## Abstract

Stability of flexible pipe relies on support from the surrounding soil. For corrugated profiles, local and distortional buckling of corrugations can limit the capacity of the pipe, though for typical profiles global buckling will dominate. This paper continues the work presented by the authors to investigate the effects of nonlinear soil support on the stability of buried corrugated metal pipes. The study presents parametric finite elements models of the buried pipe. Sliding and separation of the soil from the pipe surface, and nonuniform soil compaction are included in the analysis, and their effect on the stability of the pipe are determined. The study covers a range of typical diameters, profiles, for typical soil stiffnesses.

Keywords: Corrugated metal pipe (CMP), Buried pipe, Structural stability, Finite element analysis, Buckling.

## 1. Introduction

Stability of flexible pipe relies on support from the surrounding soil. For corrugated profiles, local and distortional buckling of corrugations can limit the capacity of the pipe, though for typical profiles global buckling will dominate. This study continues the work by the authors (Cranston et al., 2016) to investigate the effects of nonlinear soil support on the stability of buried corrugated metal pipes, through a finite element analysis of the lightest gauge of each of the annular profiles defined in ASTM A796. The analyses include sliding and separation of the soil from the pipe surface, soft haunches, and nonuniform soil compaction.

## 2. Variability of Soil Properties

The analysis presented herein includes variable soil compaction around the circumference of the pipe. Most pipe design procedures assume uniform compaction around the pipe, however this is rarely the case in installed pipe. Installations often result in variations around the circumference of the pipe and along the length of the pipe. A number of sources of this variability are outlined below:

- Haunch Zone: The pipe haunch is defined as the area of backfill soil below the lower half of the pipe between the springline and bottom of the pipe. Pipe haunches are notoriously difficult to compact, especially in larger diameter pipe. If backfill material is dumped beside the pipe and then compacted, a void will likely form in the haunch area next to the pipe. Vibratory and compaction equipment are often difficult to manipulate under the pipe haunch. Installation procedures typically require that backfill material be limited to maximum 6 in. to 8 in. in the haunch zone and that

[1] S.E., M.ASCE, Simpson Gumpertz & Heger Inc., <prgcranston@sgh.com>
[2] P.E., M.ASCE, Simpson Gumpertz & Heger Inc., <mcrichie@sgh.com>
[3] Assistant Professor, University of Campinas, <vieira@fec.unicamp.br>

material be rodded or shovel sliced to push material into the haunches and generate adequate backfill support (AASHTO, 2016) and see Figure 1. For modeling purposes, backfill support in the pipe haunch area is often modeled as a softer material representative of the difficulty in getting uniform material support and achieving desired compaction.

- Bedding: For the bedding material directly under the pipe, it is common the leave a narrow width of uncompacted soil directly under the pipe in order to avoid hard points and allow the curved bottom to conform the soil reducing voids under the haunch. In addition, the National Corrugated Steel Pipe Association (NCSPA, 2008) states that "Good bedding material can be viewed as a "cushion" for the conduit and should be relatively yielding when compared with the compacted material placed between the trench wall and the pipe. In this manner, a soil arch can develop over the pipe, thus reducing the load transmitted to the conduit." (AWWA, 2014)

- Corrugations: The valleys of deep corrugations can be difficult to compact and require hand-operated methods which can lead to variable compaction levels at the sides and haunches of the pipe.

- Shape Control: Corrugated metal structures are flexible and therefore susceptible to deflection during compaction of side fill. Movements of side fill during backfill or compaction can push against the sides of the pipe and cause "peaking" or "rolling" which can reduce the support under the pipe haunch. Shape control is required during installation but typical specifications allow up to 2% deflection from the original shape. This can result in some level of varying compaction under the pipe (AWWA, 2014).

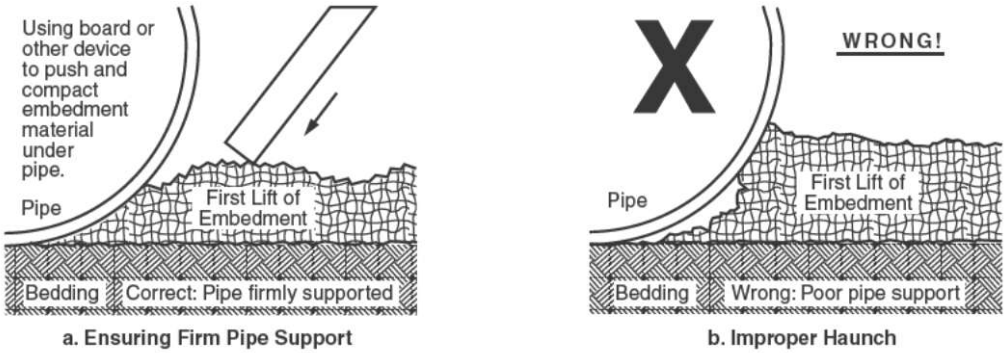


Figure 1. Haunch compaction best practice (AWWA Manual M45, 2014)

## 3. Generation of Spatially-Correlated Random Fields

To study the effect of variability in soil properties, this study introduces spatially correlated random fields for soil compaction. The following procedure is used to develop random fields with different characteristic length scales. Later in §4.3 the soil mechanical properties are defined in terms of soil compaction.

We first define a 7x7 domain, normalized by pipe diameter, with a mesh size of 0.125. The size of the domain was chosen to preclude boundary and surface effects on the response of the pipe. Since the correlation between soil mechanical properties is a function of the distance between elements, the second step is to compute a matrix of distances between elements centroids; this information is given by the Euclidean norm of a vector, represented later in Eq. 1 by $r$.

At this point, a correlation matrix that defines the correlation coefficient between every pair of element centroids has to be defined. This correlation is determined by a covariance function, also known as kernel ($k$), which specifies the covariance between random variables, in this case, the soil compaction. Many covariance functions are reported in the literature but we have chosen to use a Squared Exponential (SE) covariance function, Eq. 1. The SE covariance function is the most common and largely used covariance function, (Rasmussen and Williams, 2006). One of the benefits of using an SE covariance function is the smoothness and user control allowed by a characteristic length-scale, $\alpha$, which enables us to define a distance where the correlation between the variables is insignificant. The parameter $\alpha$ is related to the spatial frequency of variations in the field; the higher the value of $\alpha$, the higher the frequency of that variation.

$$k_{SE}(r) = e^{-\alpha r^2} \qquad \text{Eq. 1}$$

Since the correlation between elements has already been defined by the SE kernel and written in a matrix format, the soil compaction that were randomly generated – zero mean, unit variance, normally distributed, i.e. a standard Gaussian variable – can also be correlated. We generate the spatially correlated field from a singular value decomposition (SVD) of the covariance of the random field, $A$, into a left singular vector, $U$, a diagonal matrix, $S$, and a right singular vector, $V$, such that $A = USV'$. The left singular vector, U, is then multiplied by the square root of the diagonal matrix, S, and the vector of uncorrelated standard Gaussian variables, producing a stochastic field possessing the prescribed covariance function. Figure 2 depicts examples of stochastic fields with different length-scale factor and scaled to the respective variable mean and variance.

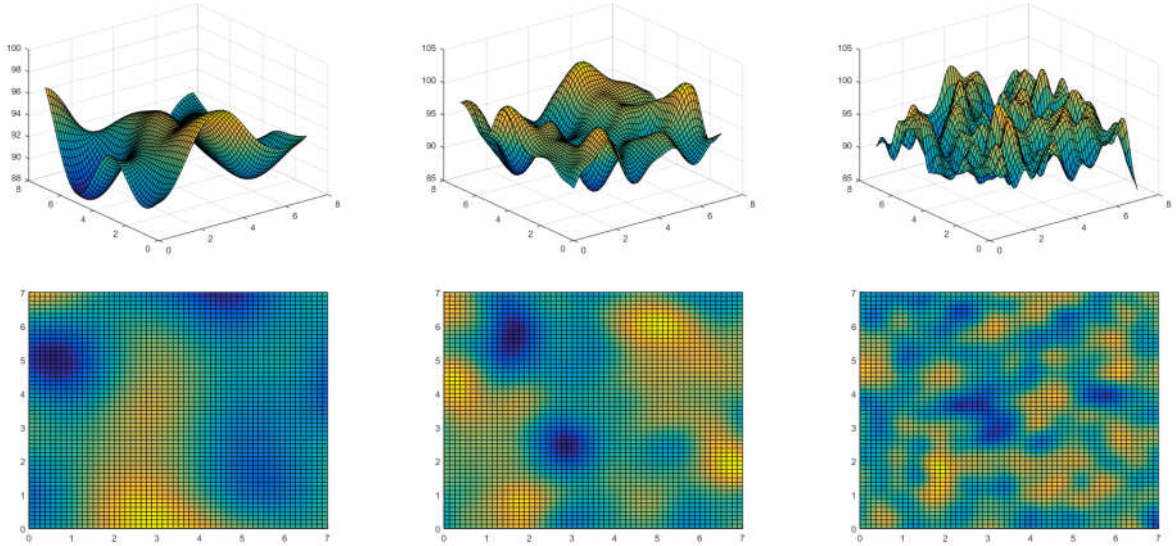

$\alpha = \frac{1}{4} \times Diameter$ $\alpha = 1 \times Diameter$ $\alpha = 4 \times Diameter$

Figure 2. Spatially correlated stochastic fields for three different length scales normalized by pipe diameter

## 4. Finite Element Analysis

In the authors' previous paper (Cranston et al., 2016), linear eigenvalue buckling analyses were performed for all annular profiles defined in the standard ASTM A796. In those linear analyses, soil was considered as an infinite elastic medium fully bonded to the pipe. Here, we refine the representation of the soil support

Table 1 - Corrugation profiles analyzed. Collected from annular profiles defined in ASTM A796.

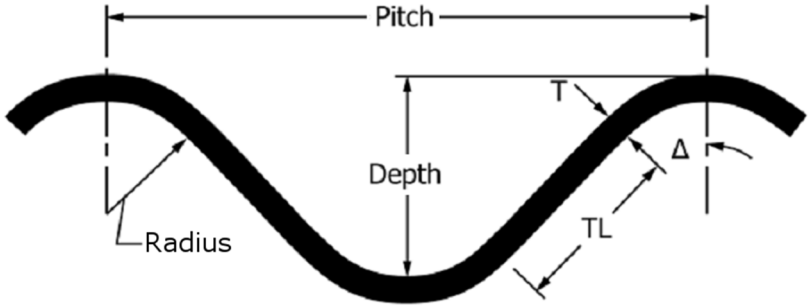


| Profile ID | ASTM A796 Ref. | Pitch | Depth | Radius | Thickness | TL | Δ | Area | Moment of Inertia | Radius of Gyration |
|---|---|---|---|---|---|---|---|---|---|---|
| | | mm | mm | mm | mm | mm | deg. | $mm^2/mm$ | $mm^4/mm$ | mm |
| 1 | Table 5 | 67.7 | 12.7 | 17.5 | 1.02 | 19.9 | 26.56 | 0.984 | 18.39 | 4.232 |
| 2 | Table 7 | 76.2 | 25.4 | 14.3 | 1.32 | 24.2 | 44.39 | 1.505 | 112.94 | 8.661 |
| 3 | Table 9 | 125 | 26 | 40 | 1.63 | 18.5 | 35.58 | 1.681 | 145.03 | 9.289 |
| 4 | Table 33 | 152.4 | 50.8 | 28.6 | 2.82 | 48.08 | 44.47 | 3.294 | 990.06 | 17.3 |
| 5 | Table 35 | 381 | 139.7 | 76.2 | 3.56 | 110.8 | 49.75 | 4.784 | 11710.7 | 49.48 |
| 6 | Table 37 | 500 | 237 | 80 | 7.11 | 198.8 | 55.7 | 10.627 | 70803.75 | 81.62 |

by introducing soil nonlinearity and nonuniformity and pipe-soil contact with sliding friction and separation. The general arrangement of the pipe-soil system is shown in Figure 3. The depth of cover and width of the model were chosen to eliminate surface and edge effects, respectively. For all analyses, we applied surcharge loading to the ground surface as an imposed displacement. We recorded the springline thrust as a measure of the load in the pipe and vertical diameter change as a measure of displacement of the pipe. We performed the analyses using the commercial finite element program ABAQUS 2016.

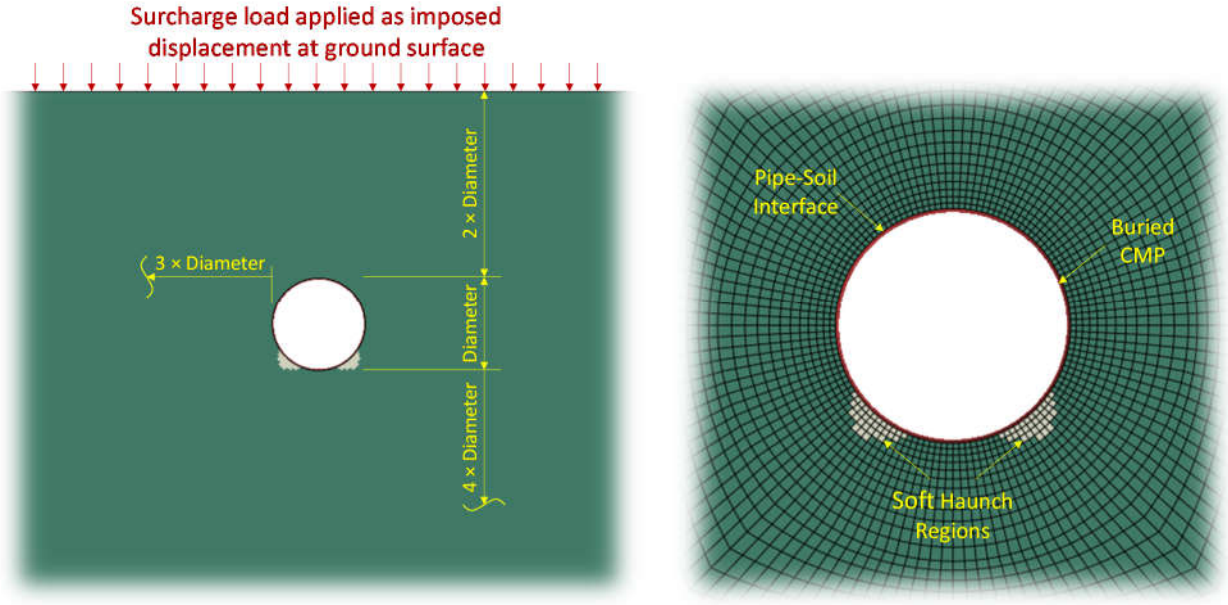


Figure 3. General arrangement of the buckling analysis of buried CMP

We performed the following sets of analyses, the details of which are presented in the subsequent subsections:

1. Plane strain analysis with uniform soil properties.
2. Plane strain analysis with soft hunches.
3. Plane strain analysis with spatially varying soil properties, 3 realizations.

We analyzed the lightest gauge of each of that annular profiles defined in ASTM A796, and the properties of those sections are shown in Table 1. We omitted the heavier gauges from the study to reduce the scope of the analysis and permit more realizations of spatially varying random soil properties, and because the results for the lighter gauges can be safely extrapolated for heavier gauges.

### *4.1. Plane strain analysis with uniform soil properties*

We first performed plane strain analyses of the response of buried pipes under surcharge loading with uniform soil properties. For each profile in Table 1, we analyzed 11 diameters, logarithmically spaced, intended to produce gross section failure modes ranging from yield to plastic instability, to elastic instability. We performed a total of 66 runs.

We modeled the pipe using 2-node linear shear flexible beam elements B21. Two corrugations of the profile were modelled using beam elements with arbitrary sections integrated during the analysis. Plasticity with hardening was defined for the pipe based on tensile tests of coupons cut from the flat portions of (something or other), and the stress strain curve is shown in Figure 4. We modeled the soil using 4-node linear plane strain elements CPE4. The soil properties are appropriate for an SW95 backfill material, which is often specified for long span CMP installations. Mohr-Coulomb soil plasticity was used. The soil properties for several compaction levels are shown in Table 2. The constitutive width of the soil was set equal to twice the pitch of the corrugation of the profile matching the width of the pipe section modeled.

Table 2. SW soil properties by compaction level

| Compaction (% Std. Proctor) | Constrained Modulus (MPa) | Soil Internal Friction Angle |
|---|---|---|
| 85 | 3.93 | 30 |
| 90 | 11.2 | 33 |
| 95 | 20.7 | 37 |
| 100 | 29.0 | 40 |

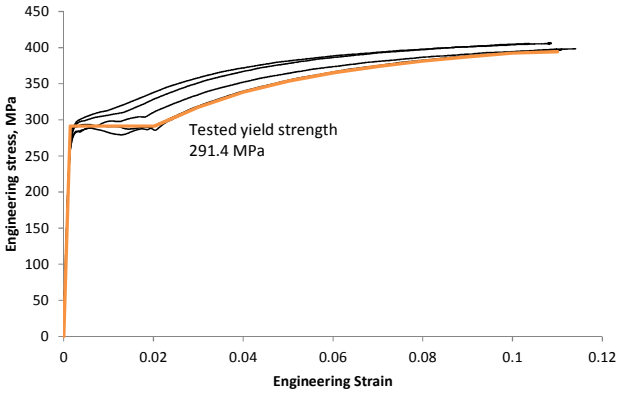


Figure 4. CMP stress-strain response from tensile tests

We modeled the pipe-soil with large displacement sliding friction contact. The pipe-soil friction coefficient was assumed to be $\mu = 0.3$. The contact definition allows the pipe to separate from the soil or slide relative to it.

For each run we applied a vertical surcharge load as an imposed displacement at the ground surface. The ground surface displacement was increased until the analysis failed to converge, usually due to numerical instability in the soil material arising severe mesh distortion at large deformations. We extracted load-displacement histories for each run, identified the onset of plastic deformation in the pipe, and identified the peak load reached during the analysis. A clearly identifiable peak load was reached for most runs.

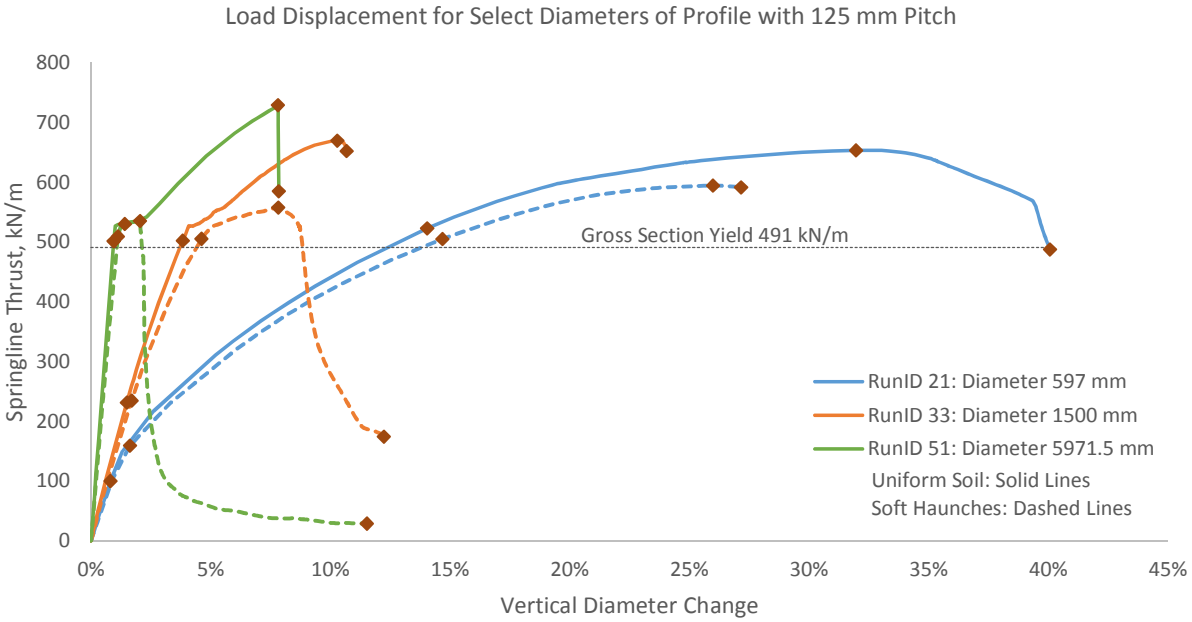


| | Diameter 597 mm | | Diameter 1500 mm | | Diameter 5972 mm | |
|---|---|---|---|---|---|---|
| | Uniform | Soft Haunch | Uniform | Soft Haunch | Uniform | Soft Haunch |
| First Yield | 0.8%, 100 kN/m | 0.6%, 71 kN/m | 1.5%, 231 kN/m | 1.7%, 234 kN/m | 1.0%, 501 kN/m | 0.8%, 361 kN/m |
| Full Section Yield | 14.1%, 523 kN/m | 14.7%, 505 kN/m | 3.8%, 502 kN/m | 4.6%, 505 kN/m | 1.0%, 501 kN/m | 1.1%, 509 kN/m |
| Max Thrust | 32.0%, 653 kN/m | 26.0%, 594 kN/m | 10.3%, 669 kN/m | 7.8%, 557 kN/m | 7.8%, 729 kN/m | 2.1%, 535 kN/m |
| Final State | 40.1%, 487 kN/m | 27.2%, 591 kN/m | 10.7%, 652 kN/m | 12.2%, 174 kN/m | 7.8%, 585 kN/m | 11.5%, 28 kN/m |

Figure 5. Load-displacement history of profile with 125 mm pitch for select diameters, plotted as springline thrust versus percent vertical diameter change. Markers indicate points of interest in the loading history, and deformed shapes with contours of plastic strain at those points are shown in the lower portion of the figure.

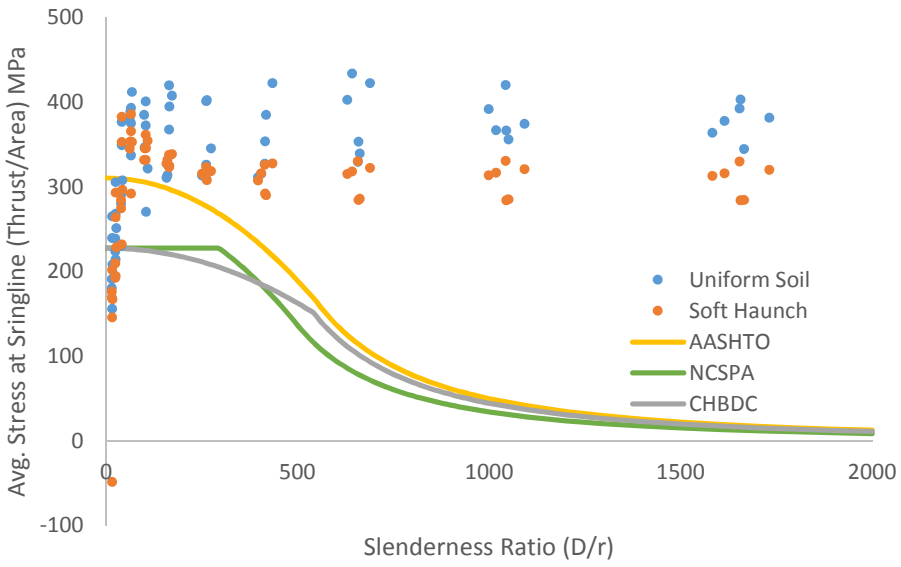


Figure 6. Capacities for analyses with uniform soil and with soft haunches, expressed as average compressive stress at springline (compressive thrust / wall area, MPa). Design curves for three common design codes are shown, demonstrating the conservative soil properties assumed in those codes.

### *4.2. Plane strain analysis with soft haunches*

We repeated the earlier uniform soil analyses but introduced an area of soft soil at the pipe haunches. We performed a total of 66 runs. As discussed in Sec. 3, the haunch soil often has lower compaction than specified. The extent of the soft haunch soil is shown in Figure 3. We assigned properties consistent with SW85 soil (representative of dumped condition backfill with little or no compaction), and these are listed in Table 2.

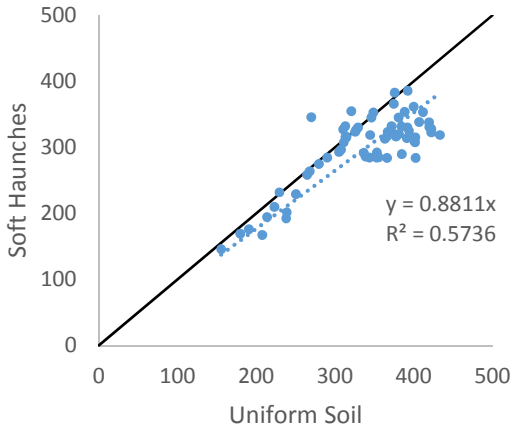


Figure 7. Capacity with Uniform Soil versus capacity with Soft Haunches

Figure 5 shows the load-displacement response and deformed shapes of the select pipe along with the deformed shapes at various stages of loading. Results are shown for companion runs with uniform soil and with soft haunches. The results show higher ductility at smaller diameters, in that the percent vertical diameter change after peak load is higher than the response of larger diameters which undergo plastic buckling. For example the pipe with 587 mm diameter undergoes plastic hinging at four locations and assumes a rectangular shape, reaching very large vertical displacements, while the pipes with 1500 and 5972 mm diameters experience a sudden drop in load carrying capacity characteristic of plastic buckling instabilities. The presence of soft haunches reduces the peak load, which is reached at a lower displacement. For larger diameters, soft haunches also reduced the load reached following the onset of pipe yield, and buckling occurred earlier in the loading history.

Figure 6 shows the peak load from each analysis plotted as a function of slenderness ratio. The capacities were governed by gross section yield except at very low slenderness ratios where bending at the pipe springline controlled (note that these designs are not efficient and not used in practice). The design curves from AASHTO, NCSPA, and CHBDC are also plotted, and the results demonstrate the conservative soil

properties assumed in those codes. Figure 7 plots the capacity calculated for uniform soil against the capacity with soft haunches, and shows a reduction in capacity for almost all cases. The average capacity reduction from the presence of soft soil in the haunch region is 12%.

### *4.3. Plane strain analysis with spatially varying soil properties*

We repeated the analyses from §4.2 with spatially varying random soil properties. To introduce soil variability into the analyses, soil physical properties were related to compaction level in terms of percent Standard Proctor compaction, as shown in Table 2. The length scale of the spatial variability is controlled by the parameter alpha. We considered five values of the parameter alpha ranging from, $D/4$ to $4D$, and examples of the compaction field are shown in Figure 2. We completed three realizations of the random soil property field for each design (profile and diameter) and scale factor alpha, for a total of 990 runs.

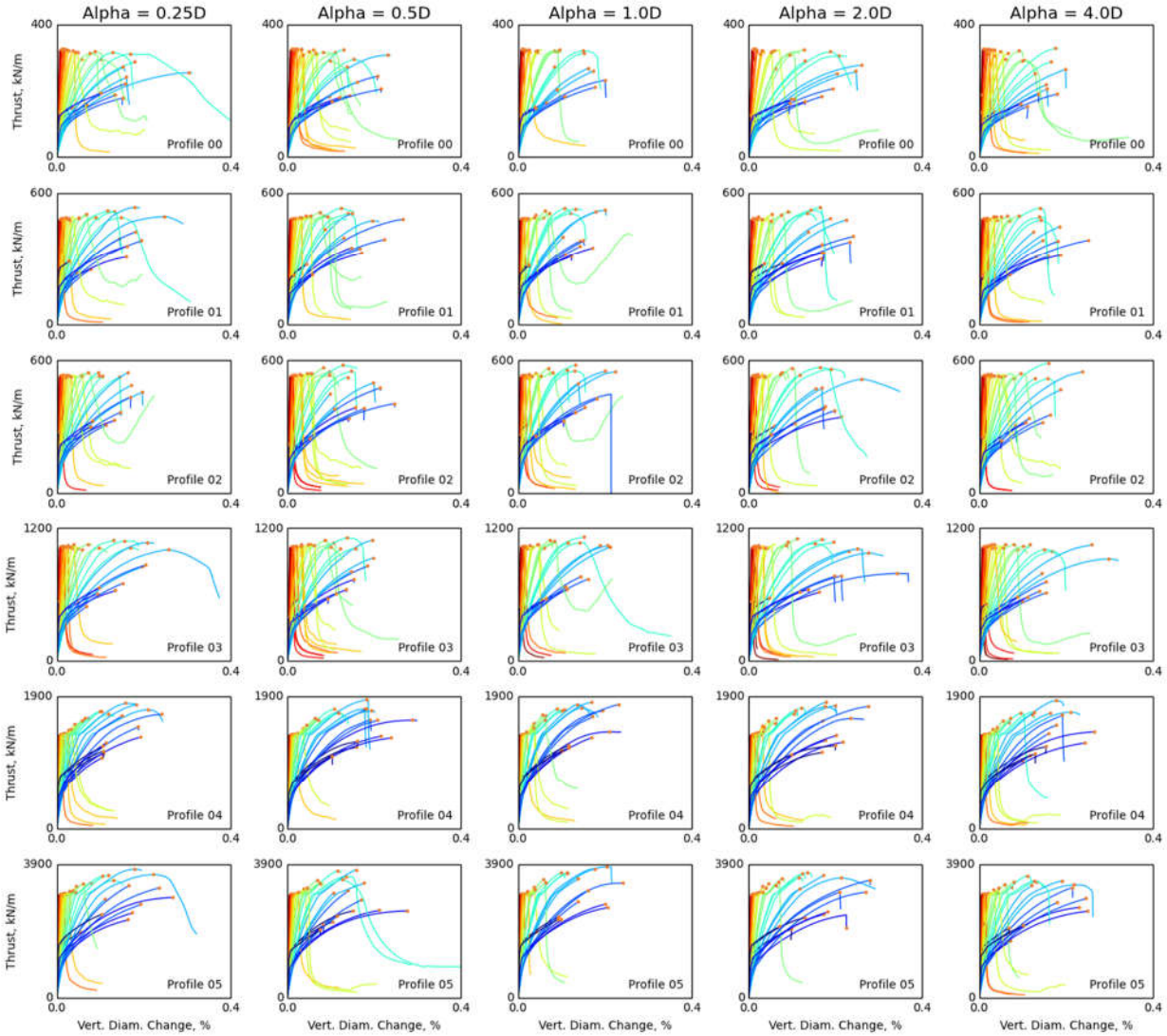


Figure 8. Load-displacement histories grouped by the profile pitch and random field scale parameter, $\alpha$, and color-coded by diameter for each profile. The smallest diameter for each profile is shown in blue and the largest diameter is shown in red. There are three realizations for each combination of profile, diameter, and $\alpha$. Peaks are identified with orange markers.

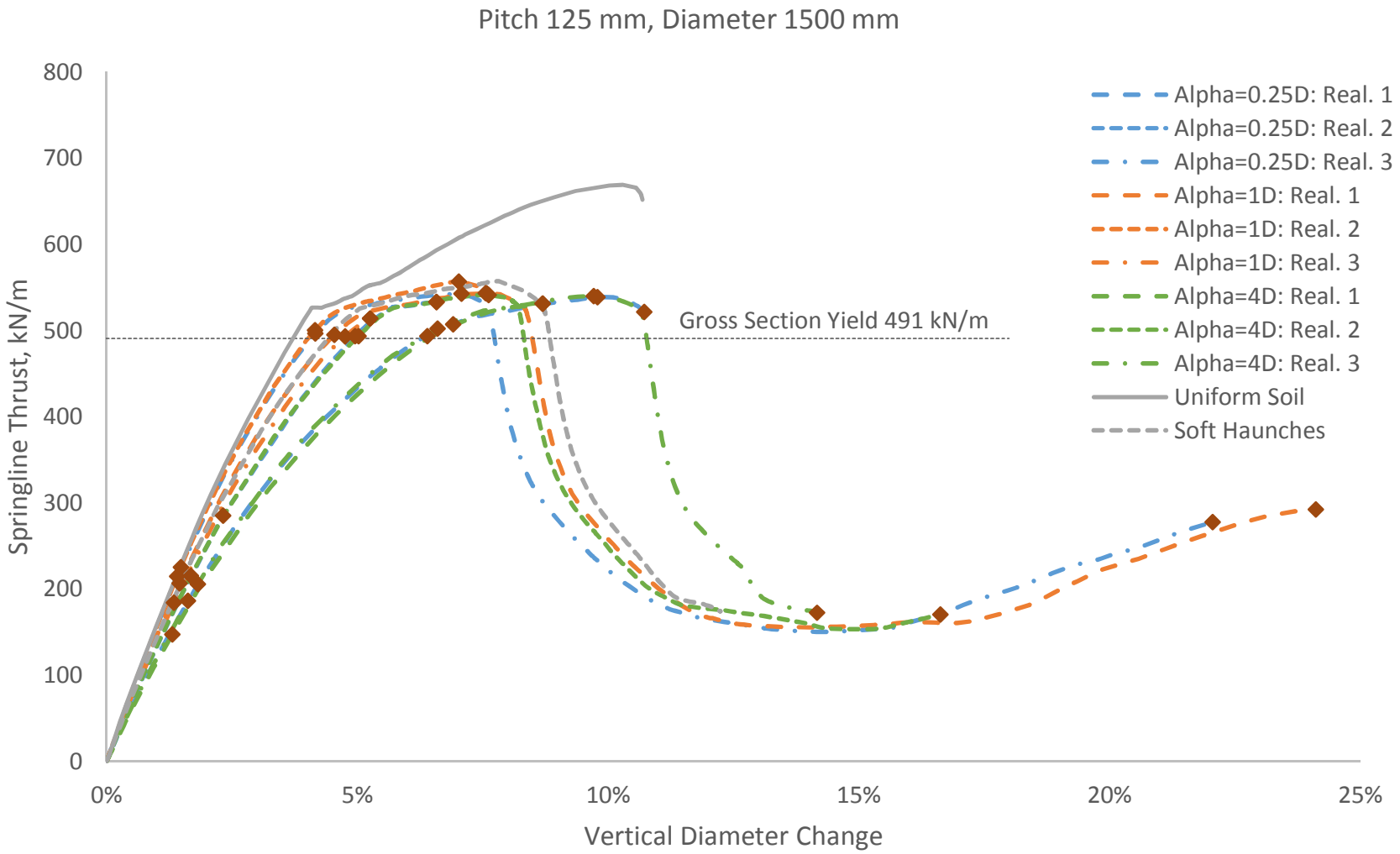


Figure 9a. Load-displacement history of profile with 125 mm pitch and 1500 mm diameter, for three realizations each of random soil compaction fields with different characteristic length scales

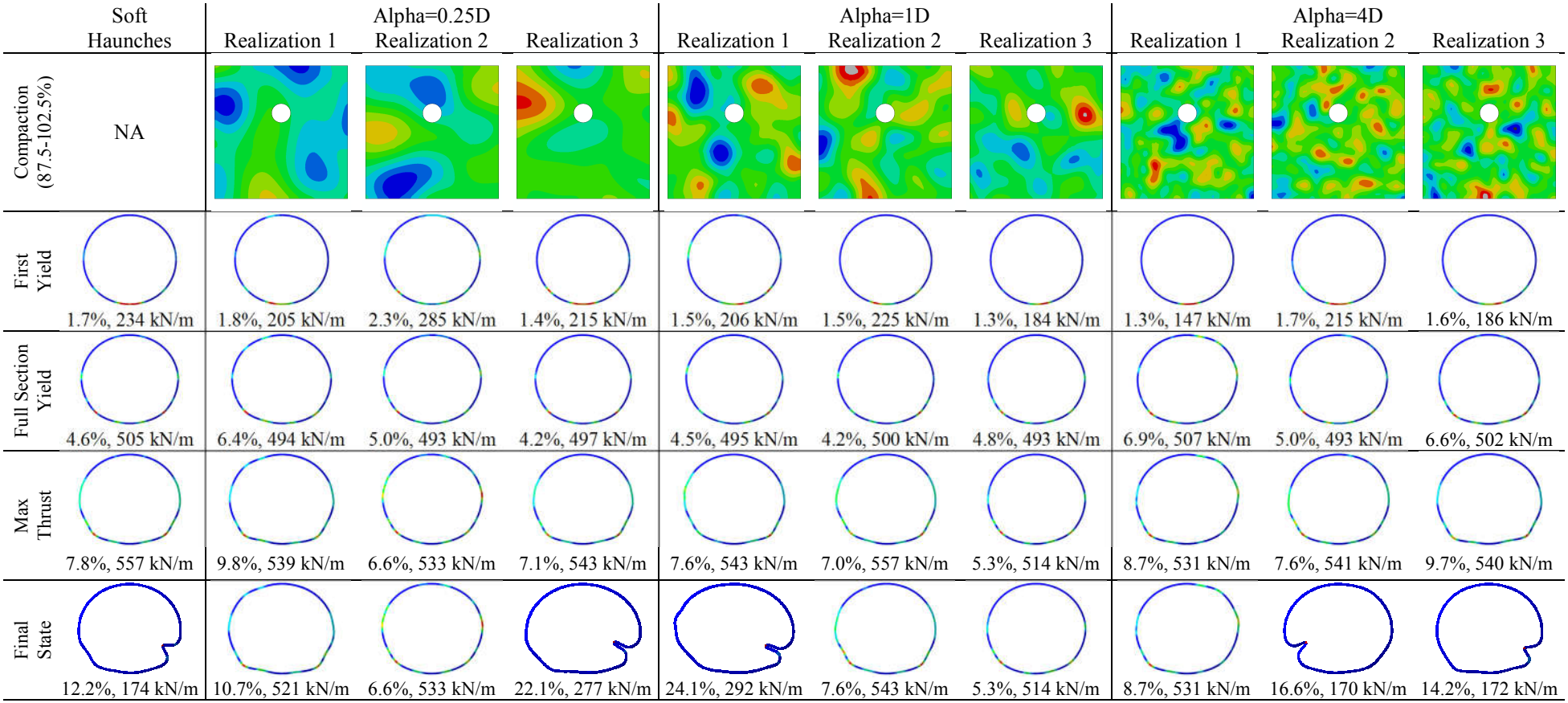


Figure 9b. Deformed shapes of profile with 125 mm pitch and 1500 mm diameter, for three realizations each of random soil compaction fields with different characteristic length scales. Contour plots show stochastic soil compaction fields for each run with a color scale between 87.5 and 102.% Standard Proctor Density.

Figure 8 shows the load-displacement results grouped by the profile pitch and random field scale parameter, $\alpha$, and color-coded by diameter. The smallest diameter for each profile is shown in blue and the largest diameter is shown in red. There are three realizations for each combination of profile, diameter, and α. Peaks are identified with orange markers. In each subfigure, the results show peak capacities below gross section compressive yield for the smallest diameters, peak capacities approximately equal to gross section yield for the largest diameters, and peak capacities higher than yield for intermediate diameters. Considered with Figure 5, the results suggest that for small diameters the failure mode is bending at springline, for intermediate diameters the failure mode is gross section yield with appreciable hardening, and for large diameters the failure mode is post-yield plastic buckling.

Figure 9 shows select deformed shapes and load-displacement responses from the study for the profile with 125 mm pitch and 1500 mm diameter for three realizations at different random field length scales. The results for deterministic soil properties are shown for reference. The results suggest that the peak load likely does not depend strongly on the scale of the soil compaction variability in the range studied, but that the displacement at peak load may be higher lowest where the characteristic length of the soil compaction variability is approximately equal to the pipe diameter.

Table 3 summarizes the calculated average and spread of the capacity, grouped by profile and random field scale parameter, calculated from three realizations analyzed for each diameter (33 runs each). The results suggest that the lowest capacity correlates to the low- and high-frequency random field (lowest and highest $\alpha$), while the highest capacities correlate to the fields with frequency on the order of the pipe diameter. Further, the results suggest that the spread of capacities (measured by standard deviation of peak compressive stress) is higher for low- and high-frequency fields and lower for fields with frequency on the order of pipe diameter. Logically, a higher-frequency random compaction field should have a smaller effect on pipe capacity. Capacity is most affected where soil-structure interaction is impacted, primarily directly along the springlines or bottom of the pipe. A review of the contour plots in Figure 9 shows that the capacities of $\alpha = 1D$ Realization 3, and $\alpha = 4D$ Realization 1 are both negatively affected by local fields of low compaction directly along the pipe. Areas of low compaction for other runs are located sufficiently away from the pipe such that we do not expect capacity to be affected by relatively small changes in compaction level. Additional realizations are needed for definitive conclusions to be made on the effect of variability in soil compaction on the stability of buried flexible pipes.

Table 3. Capacity calculated from three realizations at eleven diameters for several profiles and random soil compaction scale parameters. Capacity expressed as springline thrust divided by cross-sectional area, MPa

| Pitch, | Alpha=0.25D | | Alpha=0.5D | | Alpha=1D | | Alpha=2D | | Alpha=4D | | Trends | |
|---|---|---|---|---|---|---|---|---|---|---|---|---|
| mm | Avg | StDev | Avg | StDev | Avg | StDev | Avg | StDev | Avg | StDev | Avg | StDev |
| 67.7 | 272 | 75 | 269 | 75 | 273 | 73 | 274 | 71 | 259 | 81 | | |
| 76.2 | 289 | 62 | 290 | 58 | 294 | 54 | 294 | 53 | 283 | 65 | | |
| 125 | 274 | 64 | 279 | 62 | 286 | 58 | 283 | 59 | 271 | 72 | | |
| 152.4 | 275 | 64 | 274 | 65 | 279 | 62 | 283 | 55 | 270 | 68 | | |
| 381 | 300 | 42 | 303 | 36 | 306 | 41 | 303 | 40 | 298 | 41 | | |
| 500 | 283 | 41 | 281 | 39 | 288 | 40 | 287 | 40 | 278 | 45 | | |
| Trends | | | | | | | | | | | — | — |
| All | 282 | 59 | 282 | 58 | 288 | 56 | 287 | 54 | 277 | 64 | | |

## 5. Conclusions

This study confirmed the well-known effect of soft haunches on the stability of buried flexible pipes such as CMP. For the combinations of backfill soil and haunch soil stiffness considered, the presence of soft haunches reduced the ultimate capacity of CMP by approximately 12%, and led to earlier onset of plastic buckling.

For small diameters, the governing failure mode was bending at the pipe springline. For intermediate diameters the governing failure mode was gross-section yield, and for large diameters the governing failure mode was post-yield plastic buckling. For the combinations of profile geometry, diameter, and soil stiffness considered in this study, elastic buckling did not govern the capacity of any designs analyzed.

The effects of random fields of low compaction are not conclusive in this study. Although some trends were suggested by the results, additional realizations are warranted to arrive at defensible conclusions; the location of regions of low compaction was not sufficiently consistent for conclusions to be drawn.

## 6. Future Research

In performing this study, we identified several areas for further research. Spatially varying compaction levels should be modified to be more representative of their occurrence within the pipe backfill and embedment zone:

- Outside the backfill zone, compaction has little effects on capacity and need not include variability.
- The size of variable fields should be closely correlated to sizes that correspond to the maximum lift height for backfill.

Variable fields around the circumference of the pipe wall should be refined to correspond to the depth of corrugation to be representative of compaction difficulty within deep corrugations. Also, the analysis results should be compared with experimental data and the disparity between the results and the design code equations should be further investigated.

## References


Abaqus 2016 software documentation, Dassault Systèmes Simulia Corp., Providence, RI, USA, 2016.

AASHTO (2014), *AASHTO LRFD Bridge Design Specifications*, Customary U.S. Units, 7th Edition)

ASTM International (2015). ASTM A796 Standard Practice for Structural Design of Corrugated Steel Pipe, Pipe-Arches, and Arches for Storm and Sanitary Sewers and Other Buried Applications.

AWWA. (2008). Manual M9 Concrete Pressure Pipe, Third Edition. Denver: American Water Works Associations.

AWWA. (2004). Manual M11 Steel Pipe – A Guide for Design and Installation, Fourth Edition. Denver: American Water Works Associations.

AWWA. (2014). Manual M45 Fiberglass Pipe Design, Third Edition. Denver: American Water Works Associations.

CHBDC (2006), CSA-S6: *Canadian Highway Bridge Design Code*, Canada

Cranston, P.G., M.C. Richie, L.C.M. Vieira Jr. (2016), "Stability of Buried Corrugated Metal Pipe", Proceedings of the Annual Stability Conference, Structural Stability Conference, Orlando, FL.

NCSPA. (2008). Corrugated Steel Pipe Design Manual. Dallas: National Corrugated Steel Pipe Association

Rasmussen, C.E. and C.K.I. Williams. Gaussian Processes for Machine Learning. The MIT Press, 2006.